Article

A Dual-Emission Fluorescent Nanocomplex of Gold Clusters Decorated Silica Particle for Live Cell Imaging of Highly Reactive Oxygen Species

Tingting Chen, Yihui Hu, Yao Cen, Xia Chu, and Yi Lu

J. Am. Chem. Soc., **Just Accepted Manuscript** • DOI: 10.1021/ja4035939 • Publication Date (Web): 16 Jul 2013

A Dual-Emission Fluorescent Nanocomplex of Gold Clusters Decorated Silica Particle for Live Cell Imaging of Highly Reactive Oxygen Species

Tingting Chen,[†] Yihui Hu,[†] Yao Cen,[†] Xia Chu,*[,†] and Yi Lu*[,‡]

[†] State Key Laboratory of Chemo/Bio-Sensing and Chemometrics, College of Chemistry and Chemical Engineering, Hunan University, Changsha, 410082, P. R. China

[‡] Department of Chemistry, University of Illinois at Urbana-Champaign, Urbana, IL 61801

ABSTRACT: A novel nanocomplex displaying single-excitation and dual-emission fluorescent properties has been developed through a crown-like assembly of dye-encapsulated silica particles decorated with satellite AuNCs for live cell imaging of highly reactive oxygen species (hROS), including •OH, ClO^- and $ONOO^-$. The design of this nanocomplex is based on our new finding that the strong fluorescence of AuNCs can be sensitively and selectively quenched by these hROS. The nanocomplex is demonstrated to have excellent biocompatibility, high intracellular delivery efficiency, and stability for long-time observations. The results reveal that the nanocomplex provides a sensitive sensor for rapid imaging of hROS signaling with high selectivity and contrast.

INTRODUCTION

The development of fluorescent probes for visualizing reactive oxygen species (ROS), such as superoxide (O_2^-), singlet oxygen (O_2^1), hydrogen peroxide (H_2O_2), hydroxyl radical (•OH), hypochlorite (ClO^-), and peroxynitrite ($ONOO^-$), represents a significant challenge in chemical biology.[1] ROS are important signaling molecules that are generated in metabolic processes and play key roles in regulating a wide range of physiological functions.[2] Among various ROS, •OH, ClO^-, and $ONOO^-$ are considered to be highly ROS (hROS) because of their strong oxidant properties that can directly oxidize nucleic acids, proteins, and lipids, leading to potentially serious damage in living cells.[3] Over-accumulation of hROS induces oxidative stress and is associated with many pathological conditions, including cardiovascular disease, cancer, and neurological disorders.[4] Probes for visualizing hROS are useful for elucidating the biological roles and the underlying molecular mechanisms of these hROS, and thus hold the potential as medical diagnostics and research tools. Organic fluorescent probes have been commonly designed for the detection of hROS.[5] Their applications, however, are limited by their susceptibility to photobleaching, biotoxicity, and spontaneous autoxidation.[6] New probes with improved performance for hROS detection still constitute an active and challenging area in chemistry.

Gold nanoparticles (AuNPs) exhibit interesting size-dependent optical properties that can find wide applications in biomedicine.[7] When their conducting electrons are confined to dimensions smaller than the electron mean free path, AuNPs display unique surface plasmon resonance absorption.[8] AuNPs only consisting of several to tens of gold atoms are known as gold nanoclusters (AuNCs) and their size is comparable to the Fermi wavelength of the conduction electrons. The spatial confinement of free electrons in AuNCs generates discrete and size-tunable electronic transitions, resulting in molecular-scale properties such as strong photoluminescence.[9] Moreover, AuNCs have increased resistance to photobleaching and blinking, and do not contain toxic heavy metals, which is distinctly advantageous over semiconductor quantum dots.[10] These advantages make AuNCs a highly attractive fluorescent label for biological applications,[11] especially for intracellular and in vivo bioimaging.[12] However, the responsiveness of AuNCs to biological signaling molecules and their direct use as sensors for bioimaging remain largely unexplored.

Herein, we report for the first time that AuNCs synthesized using a glutathione template show a fluorescence signal sensitively and selectively responsive to hROS such as •OH, ClO^-, and $ONOO^-$. To take advantage of this exciting finding and to apply the AuNCs for visualizing and monitoring hROS in living cells with enhanced signal stability, improved biocompatibility, and extended observation time, we design a dual-emission fluorescent nanocomplex (DEFN) of AuNCs-decorated silica particle as a novel nanosensor for live cell imaging of hROS. This DEFN exhibits a single-excitation, dual-emission fluorescence property, one from the AuNCs with their fluorescence sensitively quenched in response to hROS, and the other from the silica particles acting as an internal reference. Such a combination of selective fluorescent quenching of AuNCs with high biocompatibility and stability against photobleaching of silica nanoparticles[13] offers the advantages of biocompatibility and real-time tracking ability, both features being essential for monitoring of intracellular signaling events. Moreover, this design allows us to utilize the tunable fluorescence emission band and intensity of the dye-encapsulated silica particle. With a suitable selection of the dye and its concentration as the internal reference, the DEFN can give a well-resolved, intensity-comparable dual-emission signal, thus affording a high contrast in imaging applications. Hence, based on intracellular delivery and two-color fluorescence monitoring of the DEFN, we are able to develop a novel sensitive intracellular nanosensor for imaging and monitoring of the hROS signaling in living cells with high contrast and long tracking time.

RESULTS AND DISCUSSION

Responsiveness of AuNCs to hROS. The key element of our DEFN sensor is the AuNCs decorated onto the surface of silica nanoparticles. The AuNCs were synthesized using a method based on the glutathione template.[14] The average size of the resulting AuNCs was ~2.1 nm, as revealed by transmission electron microscopy (TEM) (Figure 1a). The AuNCs

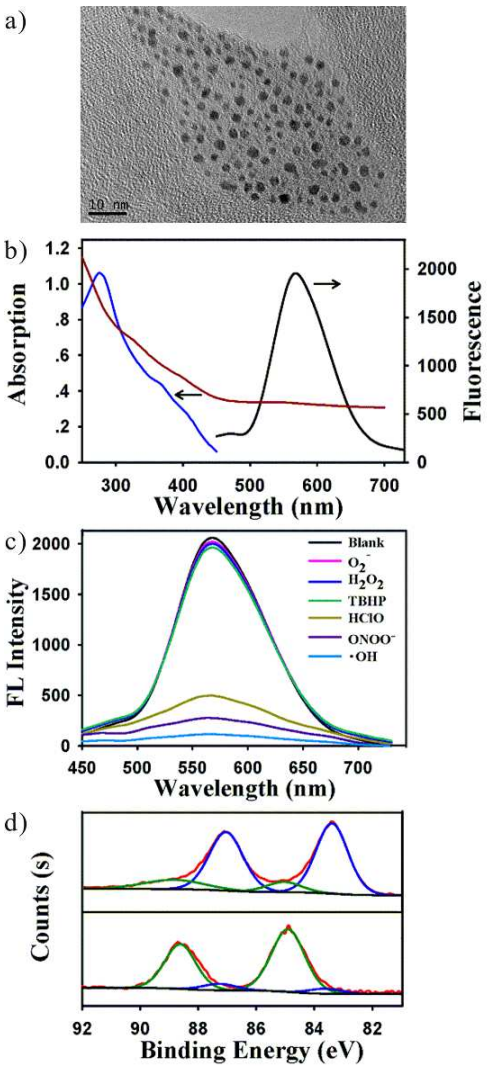

Figure 1. a) TEM of AuNCs. b) UV-vis absorption (brown), and fluorescence excitation (blue) and emission (black) spectra of AuNCs. c) Fluorescence spectral responses of AuNCs to different ROS of the same concentration (100 μM). d) XPS of AuNCs as prepared (top) and oxidized by 100 μM •OH (bottom). Raw spectra (red), deconvolution of $4f_{7/2}$ and $4f_{5/2}$ spectra into components corresponding to Au(0) (blue) and Au(I) (green).

showed a broad absorption band, with their onset near 700 nm, and emitted an intense orange fluorescence with the maximal excitation and emission wavelengths at 278 and 565 nm, respectively (Figure 1b), similar to previously reported results for glutathione-templated AuNCs.[14] In addition, the fluorescence emission at 565 nm is typical for AuNCs with smaller size.[9] The increased apparent size might indicate the as-prepared AuNCs comprise several small-size sub-clusters or the glutathione ligands have a greater effect on the HOMO-LUMO gaps of the AuNCs. A notable finding in this work was the high responsiveness of the AuNCs to ROS, especially to hROS, as shown in Figure 1c. The fluorescence of the AuNCs was significantly quenched (by 75% to 95%) in the presence of 100 μM hROS, such as ClO^-, $ONOO^-$, and •OH, while other ROS had little quenching effect (<5%) on the fluorescence of the AuNCs at the same concentration.

To elucidate the mechanism of the hROS-mediated fluorescence quenching, we analyzed the oxidation state of the AuNCs by X-ray photoelectron spectroscopy (XPS) (Figure 1d). The Au $4f_{7/2}$ spectra were deconvoluted into two distinct components corresponding to binding energies of 83.4 and 85.1 eV, which could be assigned to Au(0) and Au(I), respectively.[15] The data showed that the as-prepared AuNCs contained only a small percentage of Au(I) (~13%), which was involved in maintaining the stability of AuNCs.[16] In contrast, a large percentage of Au(I) (~93%) was obtained when the AuNCs was subjected to the reaction with hROS, such as •OH. This result indicated that the fluorescence quenching effect was attributable to oxidation of the AuNCs by hROS. More importantly, the fluorescence quenching was correlated linearly to the concentration of hROS (Figure S1 in Supporting Information), which was consistent with the quasi first-order reaction mechanism. The detection ranges were 0.2 μM to 90 μM for $ONOO^-$, 0.5 μM to 100 μM for ClO^-, and 0.03 μM to 40 μM for •OH, respectively, covering the physiological concentrations of $ONOO^-$, ClO^-, and •OH that are reported to be 1 to 50 μM, 5 to 25 μM, and 0.05 to 400 μM, respetctively.[17] Thus, the as-prepared AuNCs has adequate sensitivity for the detection of hROS under physiological conditions.

Design and Synthesis of Dual-Emission Fluorescent Nanocomplex (DEFN) for hROS Detection. To apply the AuNCs to live cell visualization of hROS signaling, the fluorescence quenching response of the AuNCs may raise the issue of giving a false signal because of unsuccessful intracellular delivery.[18] To address this issue, we designed and prepared a DEFN based on the crown nanoparticle assembly of satellite AuNCs onto a dye-encapsulated core nanoparticle, as illustrated in Scheme 1. The DEFN can be excited at a single

Scheme 1. Schematic illustration of hROS detection using the DEFN constructed by a crown nanoparticle assembly with a core dye-encapsulated silica particle and multiple satellite AuNCs.

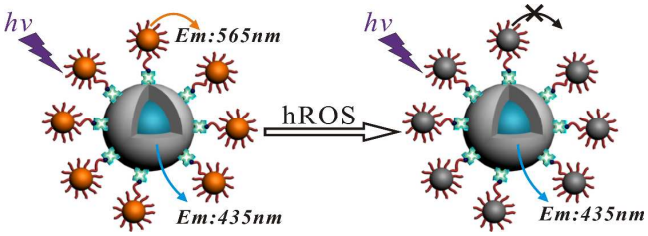

wavelength (405 nm), while emitting two differently-colored luminescent peaks, one from the AuNCs with their fluorescence sensitively quenched in response to hROS, and the other from the silica particles acting as an internal reference. This dual-emission property allows us to use the internal reference to increase imaging performance by calibrating not only the efficiency of intracellular probe delivery, but also the perturbations of operation factors, such as excitation intensity. As shown in Figure 2a, we chose CF 405S succinimidyl ester, an amine-reactive fluorescent dye with a strong and photostable emission peak well resolved from that of the AuNCs, as the encapsulated dye of the core nanoparticle. The dye was first

conjugated to 3-aminopropyl triethyloxylsilane (APTES) to obtain a silylated dye derivative (CF 405S-APTES). Then, the silica nanoparticle was synthesized using a microemulsion method by co-hydrolysis of the silylated dye and tetraethyl orthosilicate (TEOS), followed by post-coating with N-(trimethoxysilyl-propyl)-ethylenediamine triacetic acid trisodium salt (EDTAS).[19] The resulting core nanoparticle with covalently incorporated dyes was able to minimize the dye leakage.[19] The above dye-encapsulating core nanoparticles and the glutathione templated AuNCs were linked together by an oligoarginine peptide via the streptavidin (SA)-biotin and succinimide coupling chemistries. The oligoarginine peptide is known as a cell penetration peptide (CPP) that can improve the efficiency of intracellular delivery and endosomal escape of the DEFN.[20] Zeta potential measurements revealed a change of surface charge in the silica nanoparticles, from negative to positive, after they were decorated with the oligoarginine peptide conjugated AuNCs (Figure S2 in Supporting Information). This positively charged surface was generally considered beneficial for translocation of the DEFN across the plasma and endosome membranes.[20] TEM data showed the as-prepared DEFN comprised many satellite AuNCs around the silica core nanoparticle (~45 nm), clearly indicating the formation of the crown-like nanocomplex (Figure 2c). The DEFN also showed a color apparently different from that of the dye-encapsulated silica particles (Figure S3 in Supporting Information). Taken together, these data verified the successful synthesis of the crown-like nanocomplex.

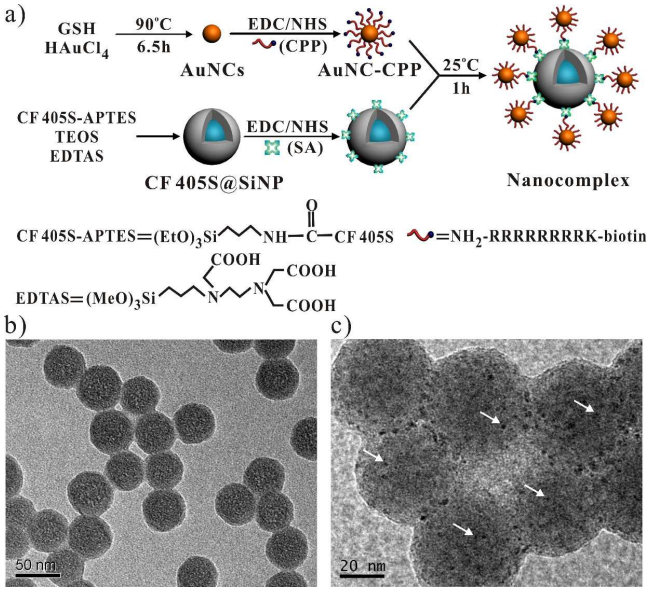

Figure 2. a) Schematic illustration of the DEFN synthesis. AuNCs are conjugated to biotinylated CPPs, dye-encapsulated core nanoparticle is modified with multiple SA, and the DEFN is obtained by crosslinking the core and satellite AuNCs via SA-biotin interaction. b) TEM of core silica nanoparticles. c) TEM of the DEFN.

***In vitro* Studies of DEFN for hROS Detection.** We then investigated the capability of the DEFN as a nanosensor for cellular hROS assays. As anticipated, the as-prepared DEFN displayed a typical dual-emission spectrum with two well-resolved fluorescence peaks, one located at 435 nm arising from the encapsulated dye, and the other at 565 nm originating from the decorated AuNCs on the surface (Figure S4 in Supporting Information). The two emission peaks were well separated with a wavelength difference of 130 nm, indicating an improved resolution for ratiometric detection and imaging analysis. When incubated with hROS for 10 min, the DEFN exhibited substantially quenched fluorescence at 565 nm, while there was little change in fluorescence intensities in the reference band at 435 nm (Figure 3a and Figure S5 in Supporting Information). Moreover, the fluorescence at 565 nm decreased with increasing hROS concentration, accompanied by a distinguishable fluorescence color change from reddish violet to blue for the DEFN (Figure 3a, inset). The ratios of

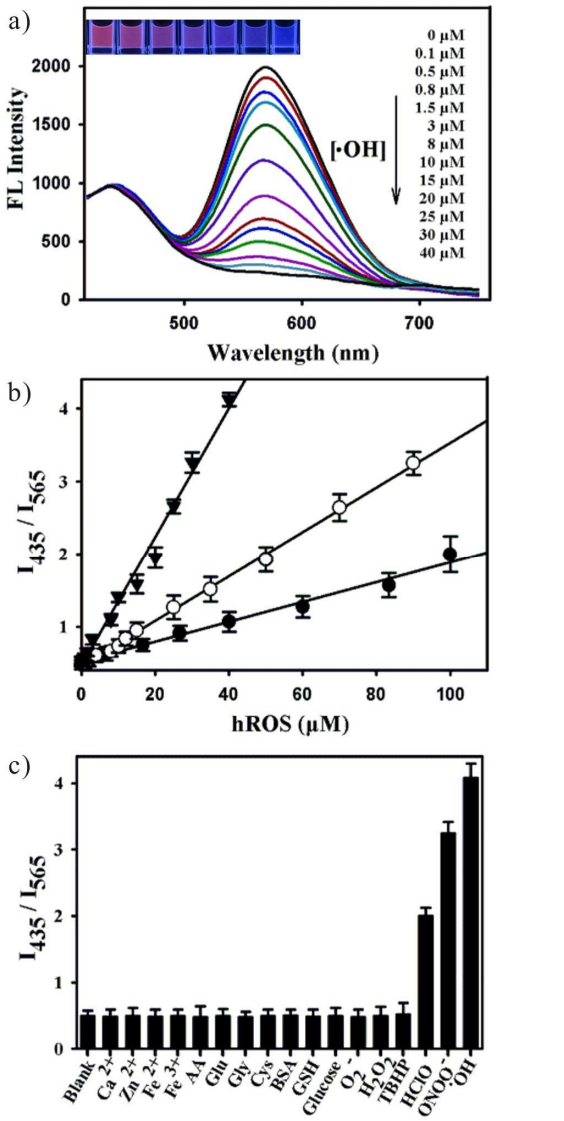

Figure 3. a) Fluorescence spectral responses of the DEFN to •OH of varying concentrations. The excitation wavelength was 405 nm. The inset is a photograph of fluorescence. b) Working curves of the DEFN-based ratiometric sensor in response to hROS. •OH (triangle), $ONOO^-$ (circle), and ClO^- (dot). c) Ratiometric responses of the DEFN sensor to hROS (100 μM ClO^-, 90 μM $ONOO^-$, and 40 μM •OH) and different coexistents (1 mM).

fluorescence intensities at 435 nm and 565 nm showed a linear relationship with increasing hROS concentrations (Figure 3b), suggesting that the DEFN acted as an ideal ratiometric sensor for quantification of hROS. The detection limits of this ratiometric sensor were 0.03, 0.2, and 0.5 μM for •OH, $ONOO^-$, and ClO^-, respectively, which cover the physiological concen-

tration ranges for the hROS, demonstrating the potential of DEFN for sensitive detection of hROS under the physiological conditions.[17] A further inspection of the fluorescence responses in the presence of other ROS and species commonly present in biological matrices revealed that these components had little quenching effect on the DEFN (Figure 3c). We ascribed this desirable selectivity to the oxidation-based mechanism of fluorescence quenching such that weak oxidants, non-oxidants and reductants in the system exert minimal interference with the fluorescence responses. These results demonstrated that DEFN holds promise as a sensitive and selective nanosensor for quantitative hROS assay.

Toxicity is a major factor to be considered in the design of an intracellular sensor system. To address this issue, we determined the degree of toxicity of the as-prepared nanocomplex using the HeLa cell line by incubating the cells with the DEFN of varying concentrations for different time intervals. Little toxicity was observed at DEFN concentrations up to 100 μg mL^{-1}, while cell viability was decreased only by ~20% for a DEFN concentration of 500 μg mL^{-1}, even after 8 h incubation (Figure S6 in Supporting Information). This result confirmed the excellent biocompatibility of the DEFN. In addition, the DEFN was found to retain its monodispersity in buffers and even in cell culture media supplemented with 10% (v/v) fetal bovine serum for over a week. This stability further supported its potential for bioimaging applications.

Live Cell Imaging of hROS with DEFN. After interrogating the *in vitro* response characteristics of the nanocomplex sensor, we then explored its ability for live cell imaging of hROS signaling. We first used HeLa cells as the model system. In this experiment, HeLa cells were first incubated with the DEFN in a serum-supplemented cell culture medium for 1 h at 37 °C. It was observed that the blue and red channels both displayed bright fluorescence signals with typical cytosolic co-localization (Figure 4a). This result indicated that the DEFN was rapidly delivered into the cytoplasm and maintained its dual-emission characteristic. With reference to a control experiment using the nanocrown assembled with a triglycine linker peptide (Figure S7 in Supporting Information), such efficient cytosolic localization of the DEFN can be attributed to our design of using the oligoarginine linker peptide that can promote cell uptake and endosomal escape. A further localization study at three different time points (15, 30 and 60 min) revealed that the DEFN was not co-localized with lysosomes, confirming cytosolic delivery of the DEFN and efficient escape from the endosomes or lysosomes (Figure S8 in Supporting Information). Moreover, the fluorescence signals from the DEFN were highly intense compared to the background from the cell, offering the possibility of high-contrast imaging. In addition, these signals remained almost unchanged for over 1 h under continuous illumination of the excitation light (Figure S9 in Supporting Information). The combination of highly intense and yet very stable fluorescence makes the DEFN an ideal candidate for real-time monitoring of the intracellular hROS signaling events with extended observation time.

Further experiments were performed by treating the DEFN-loaded HeLa cells with different ROS to examine their responsiveness. When the DEFN-loaded cells were incubated with 1 mM H_2O_2 for 10 min, we observed strong fluorescence signals at both the blue and the red channels, similar to the images obtained in the above intracellular delivery experiment (Figure 4b). This result suggested the AuNCs were not oxidized and remained highly fluorescent in this case. In contrast, a remarkable change was observed in the fluorescence images when the DEFN-loaded cells were incubated with 200 μM HClO for 5 min. The fluorescence signal almost disappeared at the red channel while the bright image was still retained in the blue channel (Figure 4c). This implied that the fluorescence of AuNCs was rapidly and substantially quenched by 200 μM HClO, providing clear evidence of fluorescence quenching-based imaging of HClO in living cells by the nanosensor.

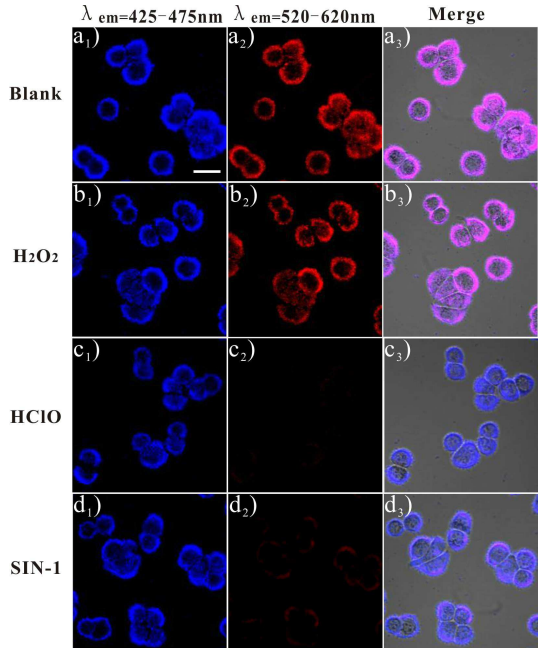

Figure 4. Confocal fluorescence microscopy images of HeLa cells treated with a) no ROS, b) 1 mM H_2O_2 for 10 min, c) 200 μM HClO for 5 min, and d) 3 mM SIN-1 for 40 min, after incubating with 75 μg mL^{-1} DEFN for 1 h at 37 °C. 1) Fluorescence images at blue channel. 2) Fluorescence images at red channel. 3) Overlap of fluorescence and differential interference contrast (DIC) images. Scale bar, 20 μm.

To validate the nanosensor's responsiveness to $ONOO^-$, we incubated the DEFN-loaded cells with 3 mM 3-morpholinosydnon-imine (SIN-1), a slow-releasing donor of $ONOO^-$.[21] In this case, a very dim fluorescence signal was obtained at the red channel after 40 min, while the blue fluorescence remained very intense, confirming the sensitive fluorescence quenching imaging of $ONOO^-$ using the DEFN (Figure 4d). Taken together, these findings revealed that the DEFN allowed selective and sensitive live cell imaging of hROS, such as HClO and $ONOO^-$, with no interference from weak ROS, such as H_2O_2. In addition, closer inspection of the temporal response of the DEFN-loaded cells treated with SIN-1 showed the red fluorescence gradually diminished with time over the 40-min imaging period (Figure S10 in Supporting Information). This observation verified the potential of the DEFN for temporal monitoring of the intracellular ROS signaling events.

Next, we applied the DEFN to another cell line model, HL-60 cells, which, when stimulated with H_2O_2, are known to produce hROS such as HClO from H_2O_2 by myeloperoxidase.[22] The cells were incubated with the DEFN in a serum-supplemented cell culture medium for 1 h at 37 °C for efficient loading of the DEFN. In this case, we also observed that both the blue and the red channels displayed strong fluorescence signals co-localized in the cytoplasm (Figure 5a). After the DEFN-loaded cells were treated with 500 μM H_2O_2 for 10

min, there was no fluorescence detected in the red channel, while the blue channel still delivered a high-contrast fluorescence image (Figure 5b). With reference to the quenching-free response for 1 mM H_2O_2 in HeLa cells (Figure 4b), we could infer the formation of hROS, such as HClO, in HL-60 cells.

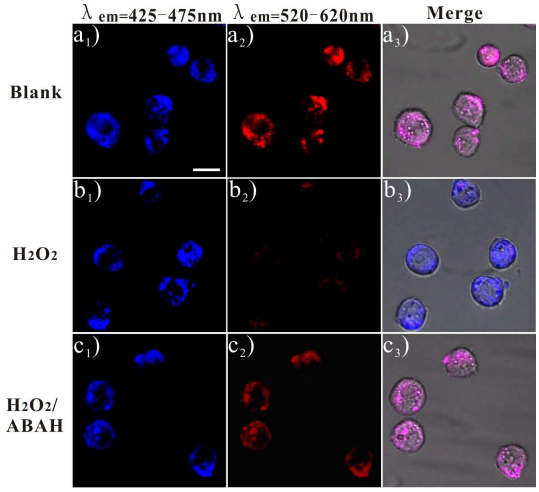

Figure 5. Confocal fluorescence microscopy images of HL-60 cells treated with a) no stimulation, b) 500 μM H_2O_2 for 10 min, and c) 500 μM H_2O_2 and 5 mM ABAH for 10 min, after incubating with 75 μg mL^{-1} DEFN for 1 h at 37 °C. 1) Fluorescence images at blue channel. 2) Fluorescence images at red channel. 3) Overlap of fluorescence and differential interference contrast (DIC) images. Scale bar, 10 μm.

Therefore, the quenched red fluorescence could be ascribed to the selective response to HClO. To validate the selectivity, a control experiment was performed by treating the DEFN-loaded cells with 500 μM H_2O_2 and 5 mM 4-aminobenzioc hydrazide (ABAH), a myeloperoxidase inhibitor known to prevent the formation of hROS,[22] for 10 min. As expected, both the red and the blue channels gave bright fluorescence images (Figure 5c), strongly suggesting that the quenched red fluorescence response was selective to the myeloperoxidase-mediated production of hROS, such as HClO. Furthermore, we performed real-time monitoring of the ROS signaling events in the HL-60 cells after varying periods of stimulation with 500 μM H_2O_2. It was observed that the fluorescence signal at the red channel decayed rapidly within 2 min and then the weak fluorescence became stabilized (Figure S11 in Supporting Information). This result indicated a fast kinetics for the ROS signaling event in the H_2O_2-stimulated HL-60 cells.

The utility of DEFN for live cell imaging of hROS signaling was further interrogated using the mouse macrophage cell line RAW264.7. Previous studies show that the macrophage cells activate the generation of hROS, such as HClO, •OH, and $ONOO^-$, after exposure to lipopolysaccharide (LPS) and phorbol 12-myristate 13-acetate (PMA).[23] In this assay, we first incubated the RAW264.7 cells with the DEFN at 37 °C for 1 h. It was observed that both the red and the blue channels displayed strong fluorescence signals (Figure 6a), an indicator for efficient internalization of the DEFN into the cells. In another case, the RAW264.7 cells were treated with 1 μg mL^{-1} LPS for 12 h, followed by co-incubation with 10 nM PMA and the DEFN at 37 °C for 1 h. Interestingly, only the blue channel delivered a bright fluorescence image while the red channel only gave a weak fluorescence signal (Figure 6b). This implied efficient fluorescence quenching of AuNCs assembled on the DEFN and suggested activation of hROS signaling in the cells. To verify that the system responds selectively to hROS, we performed a control experiment by treating the cells for 12 h with 1 μg mL^{-1} LPS and 5 mM 2,2,6,6-tetramethyl-piperidine-N-oxyl (TEMPO), a superoxide dismutase mimic that can

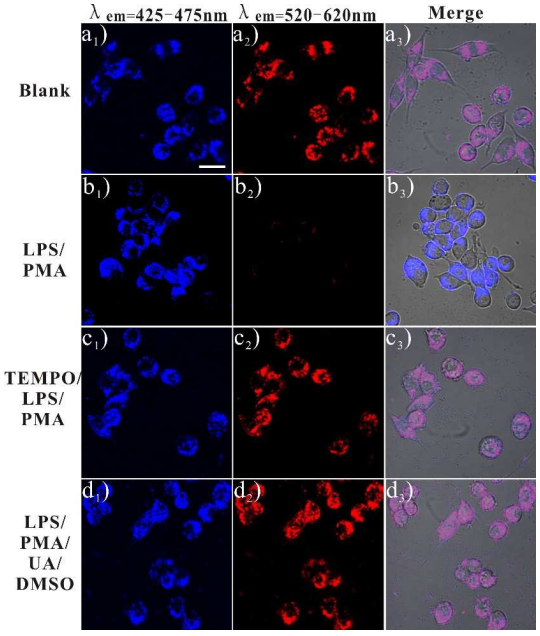

Figure 6. Confocal fluorescence microscopy images of RAW 264.7 cells. a) Cells incubated with 75 μg mL^{-1} DEFN for 1 h at 37 °C. b) Cells treated with 1 μg mL^{-1} LPS for 12 h, followed by co-incubation with 10 nM PMA and 75 μg mL^{-1} DEFN at 37 °C for 1 h. c) Cells treated with 1 μg mL^{-1} LPS and 5 mM TEMPO for 12 h, followed by 10 nM PMA and 75 μg mL^{-1} DEFN for 1 h. d) Cells treated with 1 μg mL^{-1} LPS and 10 nM PMA, followed by 250 μM UA and 0.5% DMSO for 15 min, and 75 μg mL^{-1} DEFN for 1 h. 1) Fluorescence images at blue channel. 2) Fluorescence images at red channel. 3) Overlap of fluorescence and differential interference contrast (DIC) images. Scale bar, 20 μm.

efficiently scavenge superoxide. Then, the cells were co-incubated with 10 nM PMA and the DEFN for 1 h. Because TEMPO can efficiently scavenge superoxide and inhibit myeloperoxidase, and thus reduce the formation of hROS,[24] the cells co-treated with LPS and TEMPO would only have a low hROS level. As anticipated, we observed bright images at both the blue and the red channels (Figure 6c). This result verified that the fluorescence quenching response at the red channel in Figure 6b originated from the activated hROS signaling in the cells. Moreover, another control experiment was conducted to further validate the selectivity for hROS imaging by using hROS scavengers, dimethyl sulfoxide (DMSO) and uric acid (UA). DMSO can efficiently attenuate HClO and •OH, while UA can remove HClO and $ONOO^-$,[25] thereby resulting in very low levels of hROS in the cells. To this end, the RAW264.7 cells were treated with 1 μg mL^{-1} LPS for 12 h, followed by incubation with 10 nM PMA for 1 h. The cells were subsequently treated with 250 μM UA and 0.5% DMSO for 15 min, followed by incubation with the DEFN at 37 °C for 1 h. In this case, we also observed bright fluorescence images at both the red and the blue channels. This control experiment confirmed the quenched fluorescence signal at the red channel was selective for the production of hROS, such as HClO, •OH, and $ONOO^-$, revealing the ability of DEFN for imaging of hROS signaling in living cells.

CONCLUSION

We have developed a novel dual-emission fluorescent nanocomplex (DEFN) through the crown-like assembly of a core dye-encapsulated silica particle with satellite AuNCs for live cell imaging of hROS. The design of this DEFN is based on our new finding that the strong fluorescence of AuNCs is sensitively and selectively quenched by these hROS. The DEFN can be synthesized easily by crosslinking a dye-encapsulating silica nanoparticles core and satellite AuNCs, using an oligoarginine linker peptide via streptavidin-biotin chemistry. Such a structure provides a facile approach for constructing crown nanoparticle assemblies for general intracellular delivery and imaging applications. The prepared DEFN displays an ideal single-excitation, dual-emission property with two well-resolved, intensity-comparable fluorescence peaks. These features render the DEFN very attractive due to its ability to increase the imaging contrast and accuracy. *In vitro* assays reveal that the DEFN provides a sensitive and selective sensor for quantitative ratiometric detection of hROS. Live cell studies with three cell line systems show the DEFN allows rapid imaging of hROS signaling with high selectivity and contrast. Moreover, the DEFN is demonstrated to exhibit excellent biocompatibility, high intracellular delivery efficiency even in serum matrices, and superb stability for long-time observations. In view of these advantages, the DEFN may have great potential as a high-performance platform for real-time monitoring of intracellular ROS signaling events.

EXPERIMENTAL SECTION

Materials. N-[(3-Trimethoxysilyl)propyl] ethylenediamine triacetic acid trisodium salt (EDTAS) and 3-aminopropyl triethyloxylsilane (APTES) were purchased from Gelest Inc (Morrisville, PA, USA). Triton X-100, streptavidin (SA), and dimethyl sulfoxide (DMSO) were supplied by Sangon Biotech Co. Ltd (Shanghai, China). N-Hydroxy-sulfosuccin-imide (Sulfo-NHS), 1-ethyl-3-(3-dimethyl-aminopropyl) carbodiimide hydrochloride (EDC), CF™ 405S (CF 405S) succinimidyl ester, tetraethyl orthosilicate (TEOS), L-glutathione (GSH, reduced form), 3-morpholinosydnonimine hydrochloride (SIN-1), lipopolysaccharide (LPS), phorbol 12-myristate 13-acetate (PMA), 2,2,6,6-tetramethylpiperidine-N-oxyl (TEMPO), uric acid, 4-aminobenzioc hydrazide (ABAH), cytochrome C, xanthine, xanthine oxidase (XOD 1.0-2.0 U mg^{-1}), 3-(4,5-dimethylthiahiazol-2-yl)-2,5-diphenyl tetrazolium bromide (MTT assay kit), and tert-butyl hydroperoxide solution (TBHP) were obtained from Sigma Aldrich (St. Louis, MO, USA). The cell penetration peptide (CPP) NH_2-RRRRRRRRK-biotin and the control peptide NH_2-GGGK-biotin were chemically synthesized by a solid phase method from China Peptides Co. Ltd (95% purity). HeLa cells, RAW264.7 cells, and HL-60 cells were obtained from the cell bank at Xiangya Hospital (Changsha, China). Cell culture media were purchased from Thermo Scientific HyClone (MA, USA). All other chemicals were of analytical grade and purchased from Sinopharm Chemical Reagent Co. Ltd (Shanghai, China). All solutions were prepared using ultrapure water, which was obtained through a Millipore Milli-Q water purification system (Billerica, MA, USA), with an electric resistance >18.3 MΩ.

Preparation of AuNC-CPP Conjugate. The AuNCs were synthesized through reduction of $HAuCl_4$ with GSH.[14] Briefly, a fresh 6 mM glutathione aqueous solution (10 mL) was added into a 4 mM $HAuCl_4$ aqueous solution (10 mL) under vigorous stirring at 90 °C for 6.5 h. The resulting light yellow AuNCs solutions were centrifuged at 16,000 rpm for 10 min to remove large particles. The supernatants were dialyzed against ultrapure water with a dialysis membrane (10,000 molecular weight cutoff) to purify the AuNCs from non-reacted species. The AuNCs were then ultrafiltrated using an Amicon Ultra-4 filter under centrifugation at 4,500 rpm for 30 min, and re-dispersed in 5 mL of 0.1 M phosphate buffer (PB, pH 7.4). The AuNC solution was stored at 4 °C until use.

The GSH-stabilized AuNCs were subsequently conjugated to a CPP NH_2-RRRRRRRRK-biotin as followed: in a 500 μL aliquot of the AuNC solution, a 100 μL aqueous solution containing 30 mM Sulfo-NHS and 12 mM EDC was added, and the mixture was incubated for 15 min to allow the activation of the carboxyl group on the AuNCs. Then, 1 mg CPP was added to the AuNC solution and incubated for 2 h under constant stirring at 37 °C. (Note: The biotin-labeled CPP in the study can also be a mixture of biotin-labeled CPP and label-free CPP to minimize the biotin sites on the nanocomplex surface. For cell-selective delivery applications, the design can be modified by using targeting peptide instead of CPP as the linker between the Au clusters and silica particle.) The AuNC-CPP conjugates were dialyzed against ultrapure water for 24 h with a dialysis membrane (10,000 molecular weight cutoff). The resulting AuNC-CPP conjugates were diluted to 1 mL with ultrapure water and stored at 4 °C for future use. The concentration of AuNCs in the stock solution was determined by inductive coupled plasma mass spectrometry (ICP-MS) to be ~300 μg Au mL^{-1}.

Synthesis of Dye-Encapsulated Silica Nanoparticles and DEFN. The dye-encapsulated silica nanoparticles (CF 405S@SiNP) were prepared as follows:[19] In a DMF solution of 5 mg mL^{-1} CF 405S succinimidyl ester, APTES was added to a final molar ratio of 1.2:1 (APTES:dye) and allowed to react for 24 h in the dark while shaking to obtain the conjugate of CF 405S-APTES. The dye-encapsulated silica nanoparticles were synthesized using a microemulsion method. Briefly, 1.6 mL Triton X-100, 7.5 mL cyclohexane, and 1.6 mL n-hexanol were added into a 30 mL glass vial under constant magnetic stirring. Then, 490 μL of H_2O and 10 μL of CF 405S-APTES (in DMF) were added, followed by the addition of 100 μL TEOS. After stirring for 30 min, 100 μL NH_4OH was added to initiate the silica polymerization. After 24 h, carboxyl-modified silica post-coating was initiated by adding 50 μL TEOS and 100 μL EDTAS, and polymerization proceeded for another 24 h. The resulting nanoparticles were washed three times with ethanol through centrifugation and re-suspension followed by one wash with H_2O. The dye-encapsulated particles were then lyophilized, weighed, and stored in the dark.

To prepare the nanocomplex of AuNCs decorated silica particle, we first modified the silica particles with SA as follows: in a 500 μL aliquot of 1 mg mL^{-1} dye-encapsulated particles in 0.1 M PB (pH 7.4), a 100 μL aqueous solution containing 30 mM Sulfo-NHS and 12 mM EDC was added and incubated for 15 min. 1 mg streptavidin was then added and stirred for 2 h. The SA-modified particles were washed twice by centrifugation at 18,000 rpm for 10 min, re-suspended in 500 μL of 10 mM PB (pH 7.4), and stored at 4 °C until use. The concentration of dye-encapsulated particles was estimated according to the fluorescence intensity at 435 nm to be ~1 mg mL^{-1}.

The synthesis of the nanocomplex was performed using the specific interaction between biotin and SA as follows: 2 mL

AuNCs-CPP conjugate solution was mixed with 500 μL SA-modified particles (1 mg mL^{-1}) for 1 h at room temperature. (Note: The AuNCs-CPP conjugate was used in excess as compared to the amount of silica particles such that the nanocomplex could have maximized fluorescence from AuNCs, and thus displayed maximized imaging contrast for hROS. According to the fluorescence intensity of the nanocomplex at 565 nm, the concentration of dye for synthesizing silica particles was optimized such that two fluorescence peaks of the nanocomplex could have comparable intensities.) Then, the nanocomplex was washed twice by centrifugation at 16,000 rpm for 10 min and re-suspended in 0.1 M PB (pH 7.4) to remove the excessive AuNC-peptide conjugates. The nanocomplex was re-dispersed in 1 mL 0.1 M PB (pH 7.4) and stored at 4 °C for future use. The concentration of dye-encapsulated particles in this stock solution was estimated according to the fluorescence intensity at 435 nm to be ~0.5 mg mL^{-1}. The concentration of AuNCs was estimated according to the fluorescence intensity at 565 nm to be ~60 μg Au mL^{-1}. The nanocomplex was also lyophilized and weighed, and the concentration of the nanocomplex was estimated to be ~750 μg mL^{-1}.

***In vitro* Studies of DEFN for hROS Detection.** ROS were detected with the AuNCs and the DEFN. Briefly, 10 μL AuNC solution (stock solution) or 20 μL DEFN solution (stock solution) were mixed with 100 μL reaction buffer, i.e. the phosphate buffered saline (PBS: 137 mM NaCl, 2.7 mM KCl, 10 mM Na_2HPO_4, 1.8 mM KH_2PO_4, pH 7.4), containing ROS of different concentrations. After 10 min, the fluorescence spectra were measured and recorded.

To evaluate the cytotoxicity of the DEFN, we performed an MTT assay with HeLa cells treated with the nanocomplex of varying concentrations (0, 25, 50, 100, 250, and 500 μg mL^{-1}) for different times (2, 4, and 8 h) using a Triturus microplate reader. The cell viability values (%) were then estimated using the absorbances obtained in the microplate assay.

Fluorescence Imaging of ROS in Living Cells. HeLa and RAW264.7 cells were cultured in the Dulbecco's modified Eagle's medium (DMEM) supplemented with 10% (v/v) fetal bovine serum, penicillin (100 units mL^{-1}), and streptomycin (100 μg mL^{-1}) in a humidified atmosphere containing 5% CO_2. HL-60 cells were cultured in the Roswell Park Memorial Institute (RPMI) medium supplemented with 10% (v/v) fetal bovine serum, penicillin (100 units mL^{-1}), and streptomycin (100 μg mL^{-1}) in a humidified atmosphere containing 5% CO_2.

HeLa, RAW264.7, and HL-60 cells were plated on a 35-mm Petri dish with 10-mm bottom well in the culture medium for 24 h. HeLa cells were then incubated with the DEFN solution (mixture of 100 μL DEFN and 900 μL culture medium with a DEFN concentration of ~75 μg mL^{-1}) at 37 °C for 1 h for cell uptake. In the assay of HClO, the cells were washed three times, followed by the addition of 200 μM HClO in PBS (pH 7.4), and incubation for 5 min before fluorescence imaging. In the assay of $ONOO^-$, the cells were washed three times, followed by the addition of 3 mM SIN-1 in PBS (pH 7.4), and incubation for 60 min. Both end-point and time-dependent fluorescence imaging were taken in this assay.

HL-60 cells were loaded with the DEFN solution (mixture of 100 μL nanocomplex and 900 μL culture medium) at 37 °C for 1 h, then washed three times, followed by the addition of H_2O_2 (500 μM) in PBS for 10 min before fluorescence imaging. In a control test, HL-60 cells were treated with ABAH (5 mM) and H_2O_2 (500 μM) for 10 min after incubation with the DEFN solution (mixture of 100 μL DEFN and 900 μL culture medium) at 37 °C for 1 h.

RAW264.7 cells were treated with LPS (1 μg mL^{-1}) for 12 h, then co-incubated with PMA (10 nM) and the DEFN solution (mixture of 100 μL DEFN and 900 μL culture medium) at 37 °C for 1 h, followed by washing three times before fluorescence imaging. In a control assay, RAW264.7 cells were co-treated with LPS (1 μg mL^{-1}) and TEMPO (500 μM) for 12 h, then co-incubated with PMA (10 nM) and the DEFN solution (mixture of 100 μL DEFN and 900 μL culture medium) for 1 h, followed by washing three times before fluorescence imaging. In another control experiment, RAW264.7 cells were treated with LPS (1 μg mL^{-1}) for 12 h, and then incubated with PMA (10 nM) for 1 h. The cells were subsequently cultured in a medium containing uric acid (250 μM) and DMSO (0.5%) for 15 min, followed by incubation with the DEFN solution (mixture of 100 μL DEFN and 900 μL culture medium) at 37 °C for 1 h.

ASSOCIATED CONTENT

Supporting Information

Additional experimental details and other figures. This material is available free of charge via the Internet at http://pubs.acs.org.

AUTHOR INFORMATION

Corresponding Author

xiachu@hnu.edu.cn, yi-lu@illinois.edu

Notes

The authors declare no competing financial interest.

ACKNOWLEDGMENT

This work was supported by NSFC (21275045), NCET-11-0121 and NSF of Hunan (12JJ1004)

REFERENCES

(1) Miller, E. W.; Tulyanthan, O. E.; Isaciff, Y.; Chang, C. J. *Nat. Chem. Biol.* **2007**, *3*, 263-267.

(2) (a) Finkel, T. N.; Holbrook, J. *Nature* **2000**, *408*, 239-247; (b) Sun, F.; Ji, Q.; Jones, M. B.; Deng, X.; Liang, H.; Frank, B.; Telster, J.; Peterson, S. N.; Bea, T.; He, C. *J. Am. Chem. Soc.* **2012**, *134*, 305-314.

(3) (a) Dickinson, B. C.; Srikun, D.; Chang, C. J. *Curr. Opin. Chem. Biol.* **2010**, *14*, 50-56; (b) Jiang, Q.; Xiao, N.; Shi, P.; Zhu, Y.; Guo, Z. *Coordin. Chem. Rev.* **2007**, *251*, 1951-1972.

(4) (a) Shah, A. M.; Channon, K. M. *Heart* **2004**, *90*, 486-487; (b) Ohshima, H.; Tatemichi, M.; Sawa, T. A. *Biochem. Biophys.* **2003**, *417*, 3-11; (c) Barnham, K. J.; Masters, C. L.; Bush, A. I. *Nat. Rev. Drug Discovery* **2004**, *3*, 205-214; (d) Gibellini, L.; Pinti, M.; Nasi, M.; Biasi, S. D.; Roat, E.; Bertoncelli, L.; Cossarizza, A. *Cancers* **2010**, *2*, 1288-1311.

(5) (a) Kundu, K.; Knight, S. F.; Willett, N.; Lee, S.; Taylor, W. R.; Murthy, N. *Angew. Chem. Int. Ed.* **2009**, *48*, 299-303; (b) Izumi, S.; Urano, Y.; Hanaoka, K.; Terai, T.; Nagano, T. *J. Am. Chem. Soc.* **2009**, *131*, 10189-10200; (c) Yuan, L.; Lin, W.; Yang, Y.; Chen, H. *J. Am. Chem. Soc.* **2012**, *134*, 1200-1211.

(6) Wu, C.; Jin, Y.; Schneider, T.; Burnham, D. R.; Smith, P. B.; Chiu, D. T. *Angew. Chem. Int. Ed.* **2010**, *49*, 9436-9440.

(7) (a) Giljohann, D. A..; Seferos, D. S.; Daniel, W. L.; Massich, M. D.; Patel, P. C.; Mirkin, C. A. *Angew. Chem. Int. Ed.* **2010**, *49*, 3280– 3294; (b) Xu, W.; Xue, X.; Li, T.; Zeng, H.; Liu, X. *Angew. Chem. Int. Ed.* **2009**, *48*, 6849–6852; (c) Zhao, W.; Chiuman, W.; Lam, J. C. F.; McManus, S. A.; Chen, W.; Cui, Y.; Pelton, R.; Brook, M. A.; Li, Y. *J. Am. Chem. Soc.* **2008**, *130*, 3610-3618.

(8) (a) Elghanian, R.; Storhoff, J. J.; Mucic, R. C.; Letsinger, R. L.; Mirkin, C. A. *Science* **1997**, *277*, 1078-1081; (b) Lee, J. H.; Wang, Z.; Liu, J.; Lu, Y. *J. Am. Chem. Soc.* **2008**, *130*, 14217-14226; (c) Zhao, W.; Brook, M. A.; Li, Y. *ChemBioChem* **2008**, *9*, 2363-2371.

(9) Zheng, J.; Zhang, C.; Dickson, R. M. *Phys. Rev. Lett.* **2004**, *93*, 077402/1-4.

(10) (a) Baker, M. *Nat. Methods* **2010**, *7*, 957-962; (b) Liu, C.; Wu, H.; Hsiao, Y. H.; Lai, C.; Shih, C. W.; Peng, Y.; Tang, K.; Chang,H.; Chien, Y. C.; Hsiao, J. K.; Cheng, J.; Chou, P. T. *Angew. Chem. Int. Ed.* **2011**, *50*, 7056-7060; (c) Duan, H.; Nie, S. *J. Am. Chem. Soc.* **2007**, *129*, 2412-2413.

(11) (a) Li, P.; Lin, J.; Chen, C.; Ciou, W.; Chan, P.; Luo, L.; H. Hsu, Y.; Diau, E. W.; Chen, Y. *Anal. Chem.* **2012**, *84*, 5484-5488; (b) Lin, C.; Yang, T.; Lee, C. H.; Huang, S.; Sperling, R. A.; Zanella, M.; Li, J.; Shen, J.; Wang, H.;. Yeh, H. I.; Parak, W. J.; Chang, W. *ACS Nano.* **2009**, *3*, 395-401.

(12) (a) Lin, S.; Chen, N.; Sun, S.; Chang, J.; Wang, Y.; Yang, C.; Lo, L. *J. Am. Chem. Soc.* **2010**, *132*, 8309-8315; (b) Yu, M.; Zhou, C.; Liu, J.; Hankins, J. D.; Zheng, J. *J. Am. Chem. Soc.* **2011**, *133*, 11014-11017; (c) Sun, C.; Yang, H.; Yuan, Y.; Tian, X.; Wang, L.; Guo, Y.; Xu, L.; Lei, J.; Gao, N.; Anderson, G. J.; Liang, X.; Chen, C.; Zhao, Y.; Nie, G. *J. Am. Chem. Soc.* **2011**, *133*, 8617-8624; (d) Wei, H.; Wang, Z.; Zhang, J.; House, S.; Gao, Y.; Yang, L.; Robinson, H.; Tan, L.; Xing, H.; Hou, C.; Robertson, I. M.; Zuo, J.; Lu, Y. *Nat. Nanotechnol.* **2011**, *6*, 93-97.

(13) (a) Wang, L.; Tan, W.; *Nano. Lett.* **2006**, *6*, 84-88; (b)Piao, Y.; Burns, A.; Kim, J.; Wiesner, U.; Hyeon, T.; *Adv. Func. Mater.* **2008**, *18*, 3745-3758.

(14) Chen, W.; Tu, X.; Guo, X.; *Chem. Commun.* **2009**, 1736-1738.

(15) Xie, J.; Zheng, Y.; Ying, J. *J. Am. Chem. Soc.* **2009**, *131*, 888-889.

(16) (a) Whetten, R. L.; Price, R. C. *Science* **2007**, *318*, 407-408; (b) Pyykkö P. *Angew. Chem. Int. Ed.* **2004**, *43*, 4412-4456.

(17) (a) Dairou, J.; Atmane, N.; Lima, F. R.; Dupret, J. M. *J. Biol. Chem.* **2004**, *279*, 7708-7714; (b) Mancini, M. C.; Kairdolf, B. A.; Smith, A. M.; Nie, S. *J. Am. Chem. Soc.* **2008**, *130*, 10836-10837. (c) Grootveld, M.; Halliwell, B. *Biochem. J.* **1986**, *237*, 499-504; (d) Korotkova, E. I.; Misini, B.; Dorozhko, E. V.; Bukkel, M. V.; Plotnikov, E. V.; Linert, W. *Int. J. Mol. Sci.* **2011**, *12*, 401-409.

(18) Si, D.; Epstein, T.; Lee, Y. Kopelman, R. *Anal. Chem.* **2012**, *84*, 978-986.

(19) (a) Medley, C. D.; Bamrungsap, S.; Tan, W.; Smith, J. E. *Anal. Chem.* **2011**, *83*, 727-734; (b) Lee, J. E.; Lee, N.; Kim, H.; Kim, J.; Choi, S. H.; Kim, J. H.; Kim, T.; Song, I. C.; Park, S. P.; Moon, W. K.; Hyeon, T. *J. Am. Chem. Soc.* **2010**, *132*, 552-557.

(20) (a) Jiang, T.; Olson, E. S.; Nguyen, Q. T.; Roy, M. P.; Jennings, A.; Tsien, R. Y. *Proc. Natl. Acad. Sci. USA* **2004**, *101*, 17867-17872; (b) Elsabahy, M.; Wooley, K. L.; *Chem. Soc. Rev.* **2012**, *41*, 2545-2561.

(21) Yang, D.; Wang, H.; Sun, Z.; Chung, N.; Shen, J. *J. Am. Chem. Soc.* **2006**, *128*, 6004-6005.

(22) Kagan, V. E.; Konduru, N. V.; Feng, W.; Allen, B. L.; Conroy, J.; Volkov, Y.; Vlasova, I. I.; Belikova1, N. A.; Yanamala, N.; Kapralov, A.; Tyurina, Y. Y.; Shi, J.; Kisin, E. R.; Murray, A. R.; Franks, J.; Stolz, D.; Gou, P.; Seetharaman, J. K.; Fadeel, B.; Star, A.; Shvedova, A. A. *Nat. Nanotechnol.* **2010**, *5*, 354-359.

(23) (a) McQuade, L. E.; Lippard, S. J. *Curr. Opin. Chem. Biol.* **2010**, *14*, 43-49; (b) Yu, F.; Li, P.; Li, G.; Zhao, G.; Chu, T.; Han, K. *J. Am. Chem. Soc.* **2011**, *133*, 11030-11033; (c) Dickinson, B. C.; Huynh, C.; Chang, C. J. *J. Am. Chem. Soc.* **2010**, *132*, 5906-5915; (d) Gomez-Mejiba, S. E.; Zhai, Z.; Gimenez, M. S.; Ashby, M. T.; Chilakapati, J.; Kitchin, K.; Mason, R. P.; Ramirez D. C. *J. Biol. Chem.* **2010**, *285*, 20062-20071.

(24) (a) Muijsers, R. B.; Van Den Worm, E.; Folkerts, G.; Beukelman, C. J.; Koster, A. S.; Postma, D. S.; Nijkamp, F. P. *Br. J. Pharmacol.* **2000**, 130, 932-936; (b) Chatterjee, P. K.; Cuzzocrea, S.; Brown, P. A. J.; Zacharowski, K.; Stewart, K. N.; Mota-Filipe, H.; Thiemermann, C. *Kidney Int.* **2000**, *58*, 658-673.

(25) (a) Zhu, Q.; Lian, Y.; Thyagarajan, S.; Rokita, S. E.; Karlin, K. D.; Blough, N. V. *J. Am. Chem. Soc.* **2008**, *130*, 6304-6305; (b) Hooper, D. C.; Spitsin, S.; Kean, R. B.; Champion, J. M.; Dickson, G. M.; Chaudhry, I.; Koprowski, H. *Proc. Natl. Acad. Sci. USA* **1998**, *95*, 675-680.

TOC